

Environmental spaces for palsas and peat plateaus are disappearing at a circumpolar scale

Oona H. Könönen et al.

Correspondence to: Oona H. Könönen (oona.kononen@oulu.fi)

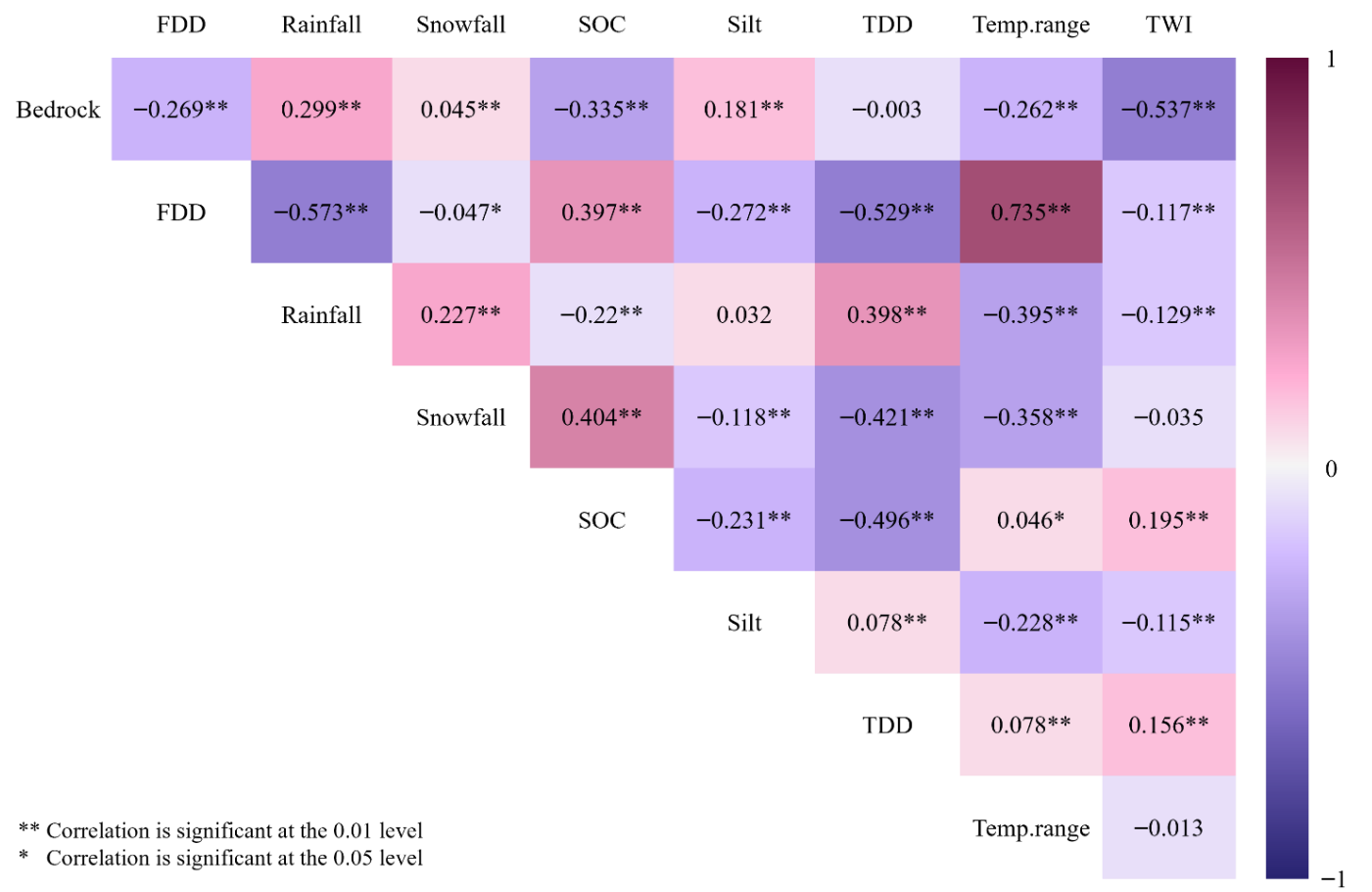
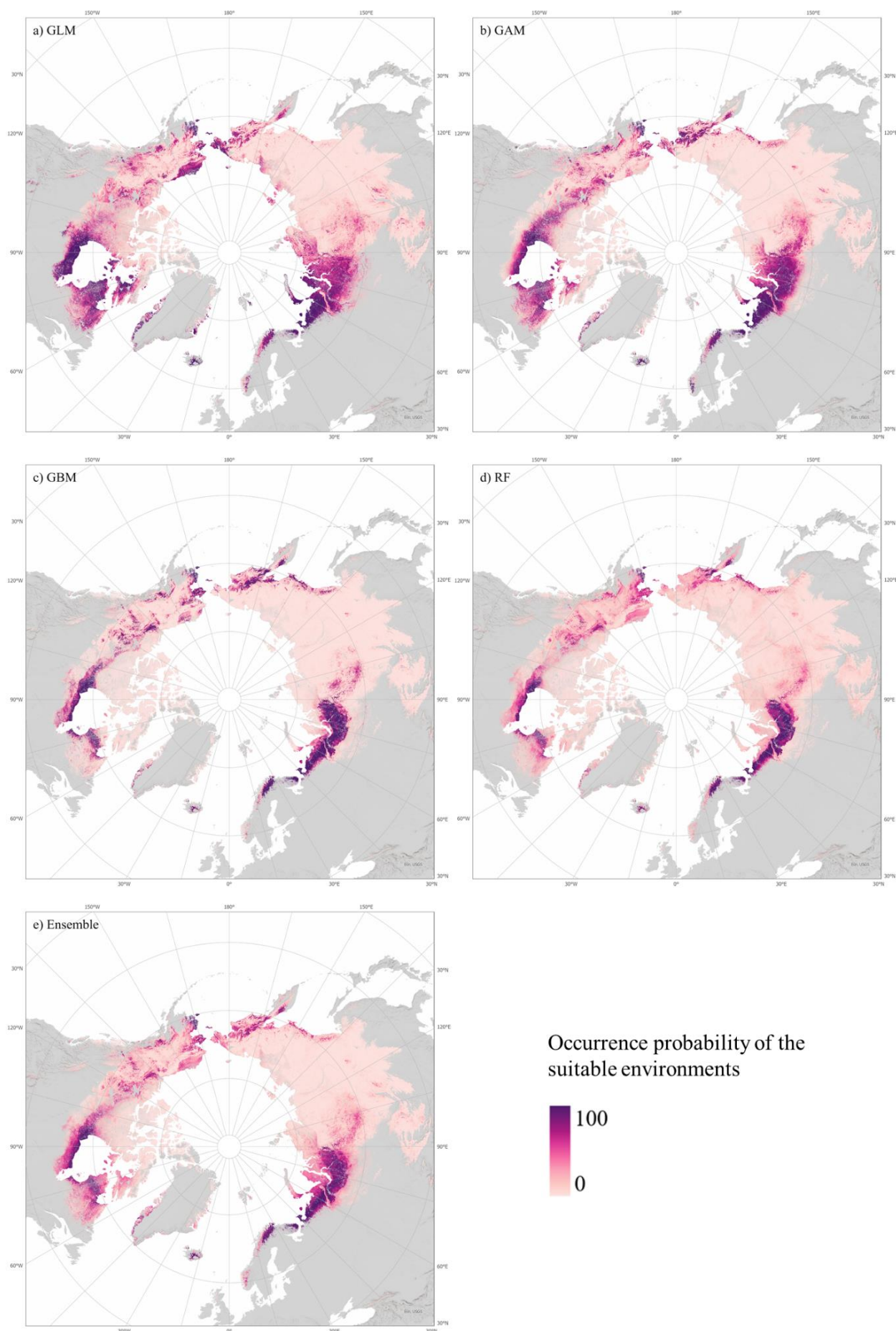


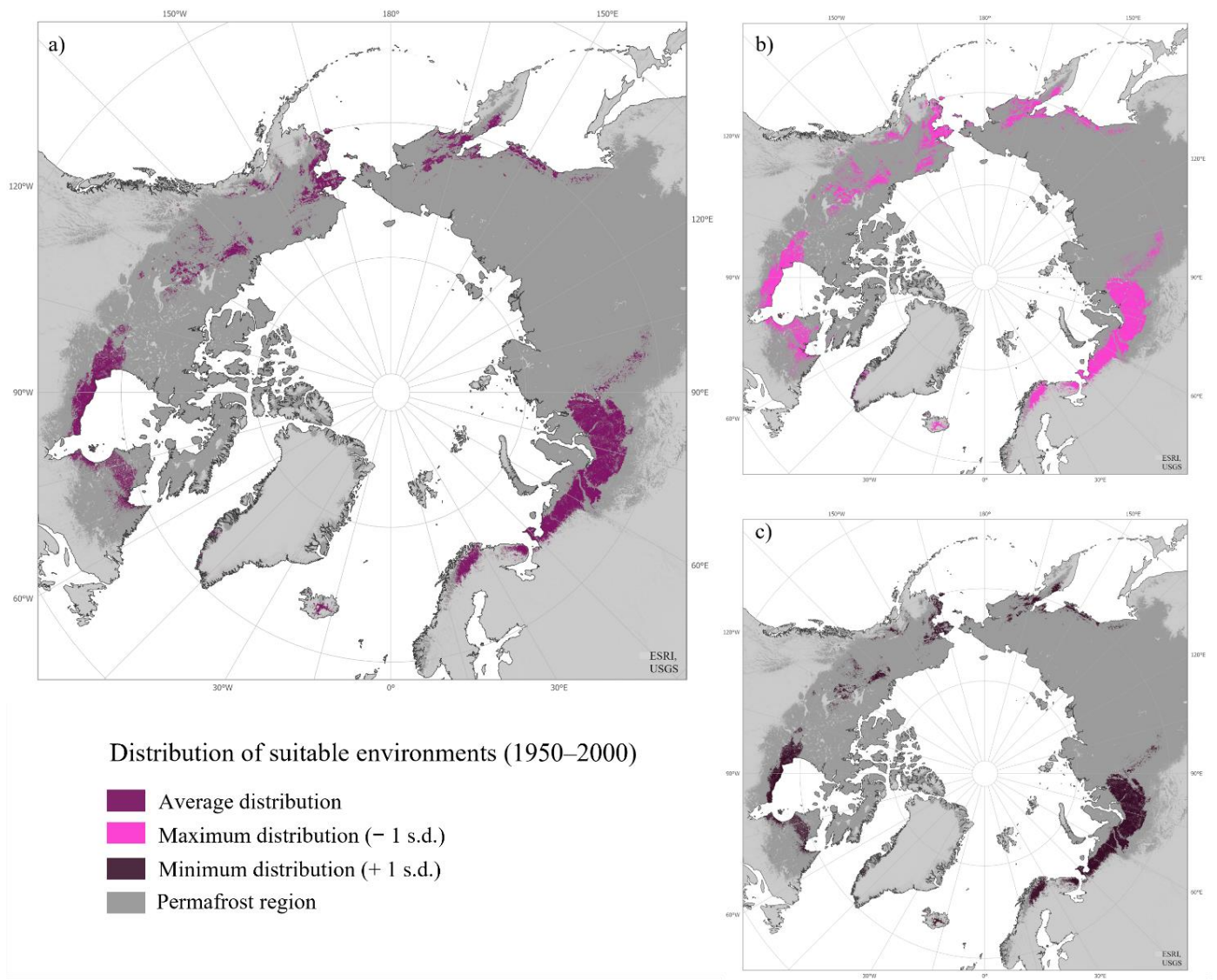
Figure S1: Bivariate correlations between used environmental variables. Spearman two-tailed correlations are color-graded (positive purple, and negative violet) according to their strength. Abbreviated variables are thawing- and freezing degree-days (TDD and FDD, °C-days), annual air temperature range (Temp.range, °C), topographic wetness index (TWI), soil organic carbon content (SOC, g kg<sup>-1</sup>), silt content (Silt, g kg<sup>-1</sup>) and bedrock probability within two meters (Bedrock, %). Statistical significance of the correlation is illustrated with \*\* p ≤ 0.01 level) and \* p ≤ 0.05.

Table S1: Average True Skill Statistic (TSS) cut-off values and ±1 standard deviations for used modelling methods (generalized linear model (GLM), generalized additive model (GAM), generalized boosting method (GBM), random forest (RF), and ensemble of the former methods). Calculations were based on 100 modelling runs of each method. Cut-off values were used in the binary classification.

	GLM	GAM	GBM	RF	Ensemble
Cut-off value	0.42 ± 0.081	0.48 ± 0.115	0.44 ± 0.166	0.45 ± 0.087	0.52 ± 0.088



**Figure S2: Occurrence probabilities of the suitable environments for the used modelling methods (a) generalized linear model (GLM), b) generalized additive model (GAM), c) generalized boosting method (GBM) and d) random forest (RF), and e) ensemble of the former methods. Model predictions are extracted for the permafrost region (Ran et al. 2022).**



**Figure S3: Comparison between binary classifications of the suitable environments (for period 1950–2000) for palsas and peat plateaus, based on different True Skill Statistic (TSS) cutoff values calculated from 100 model iterations: (a) average, (b) -1 standard deviation and (c) +1 standard deviation. On the background the permafrost region on dark grey (Ran et al. 2022).**

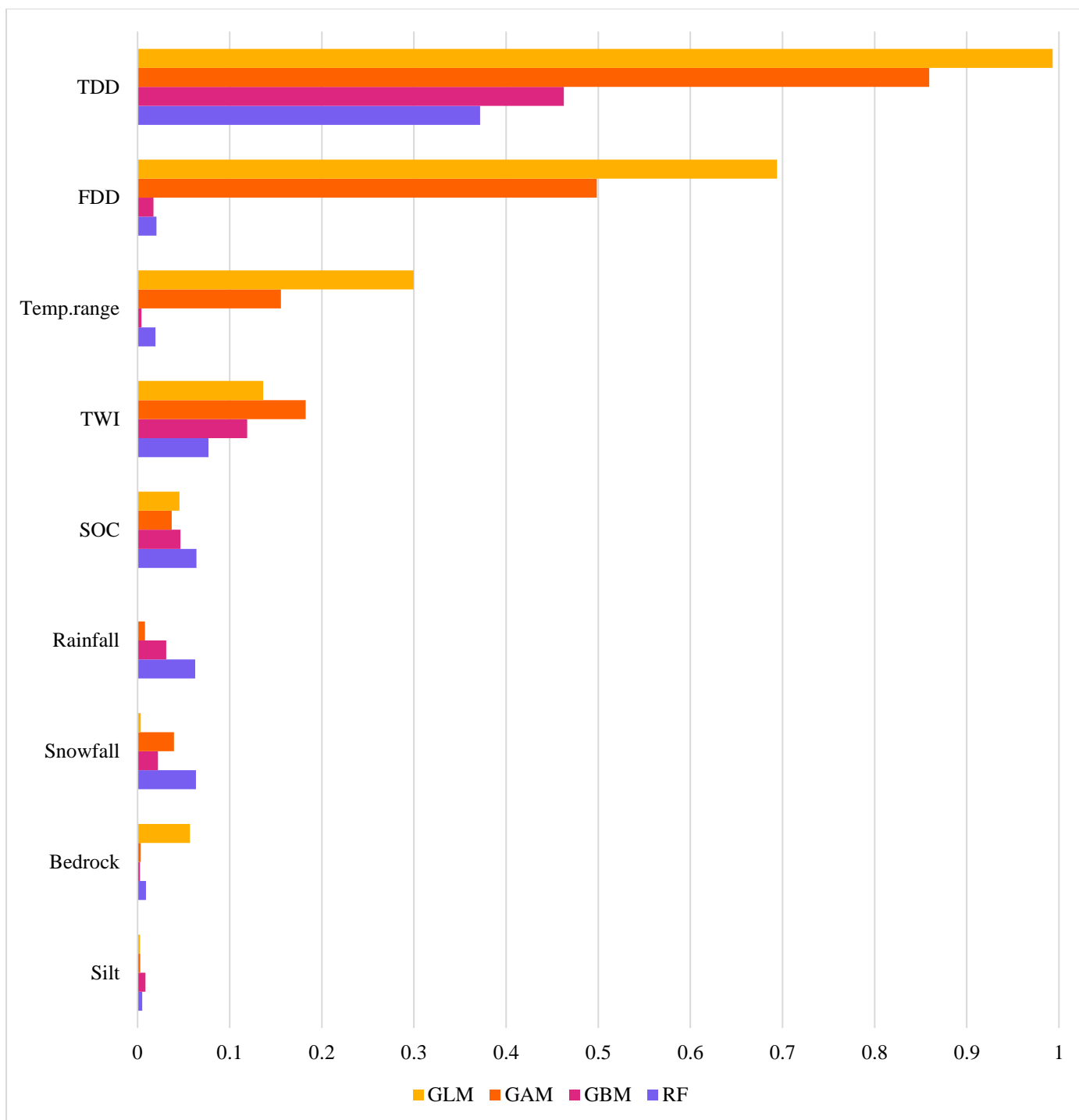


**Figure S4: Variable importance of the environmental factors in different models (generalized linear model (GLM), generalized additive model (GAM), generalized boosting method (GBM) and random forest (RF). Abbreviated variables are thawing- and freezing degree-days (TDD and FDD, °C-days), annual air temperature range (Temp.range, °C), topographic wetness index (TWI), soil organic carbon content (SOC, g kg<sup>-1</sup>), silt content (Silt, g kg<sup>-1</sup>) and bedrock probability within two meters from the ground surface (Bedrock, %).**

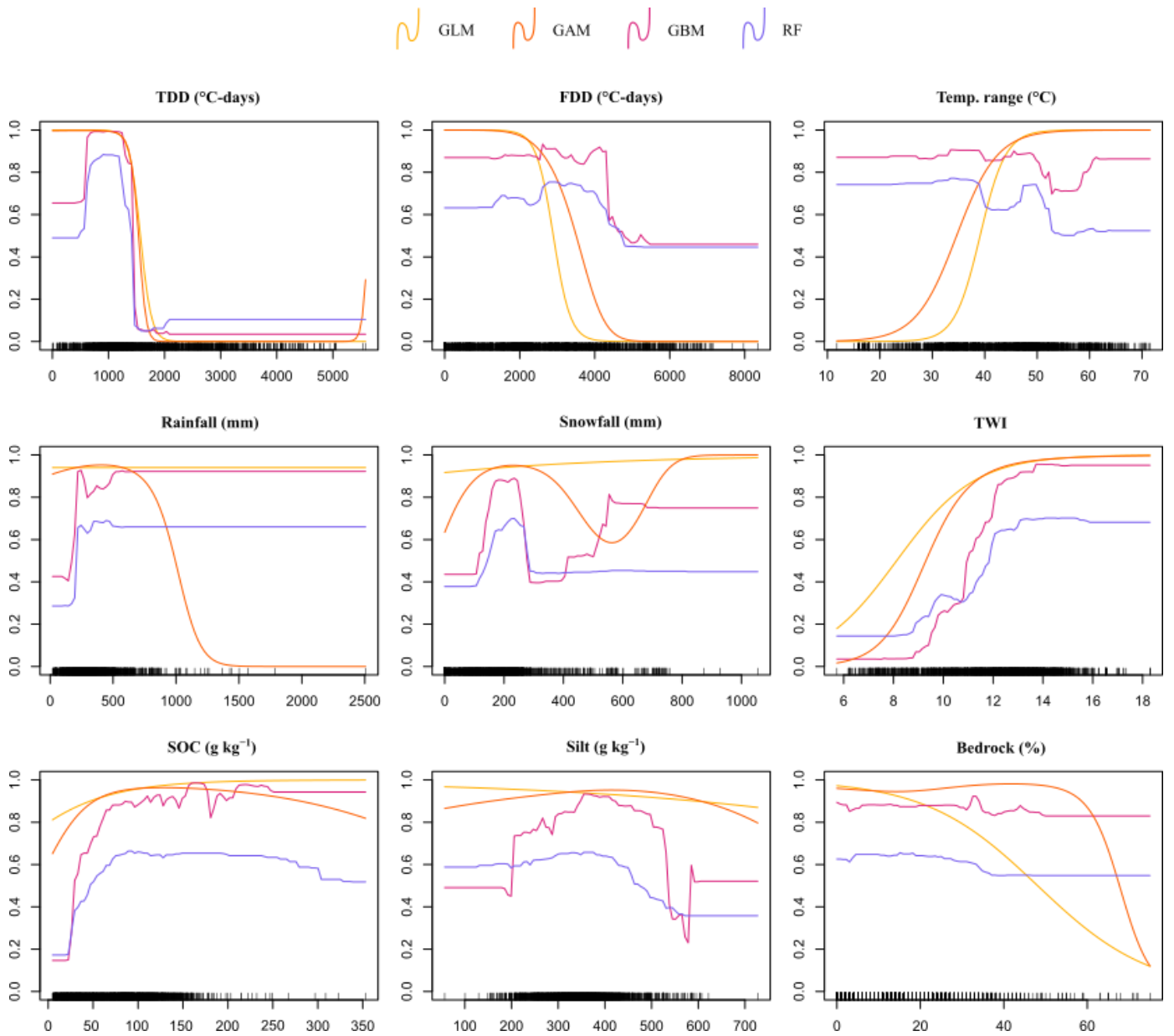


**Figure S5: Response curves of the environmental factors. Results from four used models (generalized linear model (GLM), generalized additive model (GAM), generalized boosting method (GBM) and random forest (RF)).** Abbreviated variables are thawing- and freezing degree-days (TDD and FDD, °C-days), annual air temperature range (Temp.range, °C), topographic wetness index (TWI), soil organic carbon content (SOC, g kg<sup>-1</sup>), silt content (Silt, g kg<sup>-1</sup>) and bedrock probability within two meters from the ground surface (Bedrock, %).

**Table S2: Suitable environmental environments (in km<sup>2</sup>) for palsas and peat plateaus at different time periods and representative concentration pathway (RCP) climate change scenarios for used modelling methods (generalized linear model (GLM), generalized additive model (GAM), generalized boosting method (GBM), random forest (RF), and ensemble of the former methods). Areal percentage changes are given in relation to the modelled area of period 1950–2000.**

Model	Scenario	Suitable environments (km <sup>2</sup> )	Percentage change (%)
GLM	1950–2000	3 787 750	
	RCP2.6 2041–2060	2 538 710	-33.0
	RCP2.6 2061–2080	2 465 660	-34.9
	RCP4.5 2041–2060	2 410 500	-36.4
	RCP4.5 2061–2080	2 002 450	-47.1
	RCP8.5 2041–2060	1 970 290	-48.0
	RCP8.5 2061–2080	1 257 860	-66.8
GAM	1950–2000	2 926 920	
	RCP2.6 2041–2060	1 343 190	-54.1
	RCP2.6 2061–2080	1 256 910	-57.1
	RCP4.5 2041–2060	1 151 210	-60.7
	RCP4.5 2061–2080	819 280	-72.0
	RCP8.5 2041–2060	782 370	-73.3
	RCP8.5 2061–2080	338 800	-88.4
GBM	1950–2000	2 039 920	
	RCP2.6 2041–2060	672 490	-67.0
	RCP2.6 2061–2080	637 110	-68.8
	RCP4.5 2041–2060	549 850	-73.1
	RCP4.5 2061–2080	352 040	-82.7
	RCP8.5 2041–2060	329 310	-83.9
	RCP8.5 2061–2080	103 820	-94.9
RF	1950–2000	1 587 360	
	RCP2.6 2041–2060	416 910	-73.7
	RCP2.6 2061–2080	376 650	-76.3
	RCP4.5 2041–2060	296 110	-81.4
	RCP4.5 2061–2080	169 460	-89.3
	RCP8.5 2041–2060	151 990	-90.4
	RCP8.5 2061–2080	28 590	-98.2
Ensemble	1950–2000	1 860 830	
	RCP2.6 2041–2060	622 230	-66.6
	RCP2.6 2061–2080	573 570	-69.2
	RCP4.5 2041–2060	499 720	-73.2
	RCP4.5 2061–2080	291 550	-84.3
	RCP8.5 2041–2060	268 030	-85.6
	RCP8.5 2061–2080	65 360	-96.5



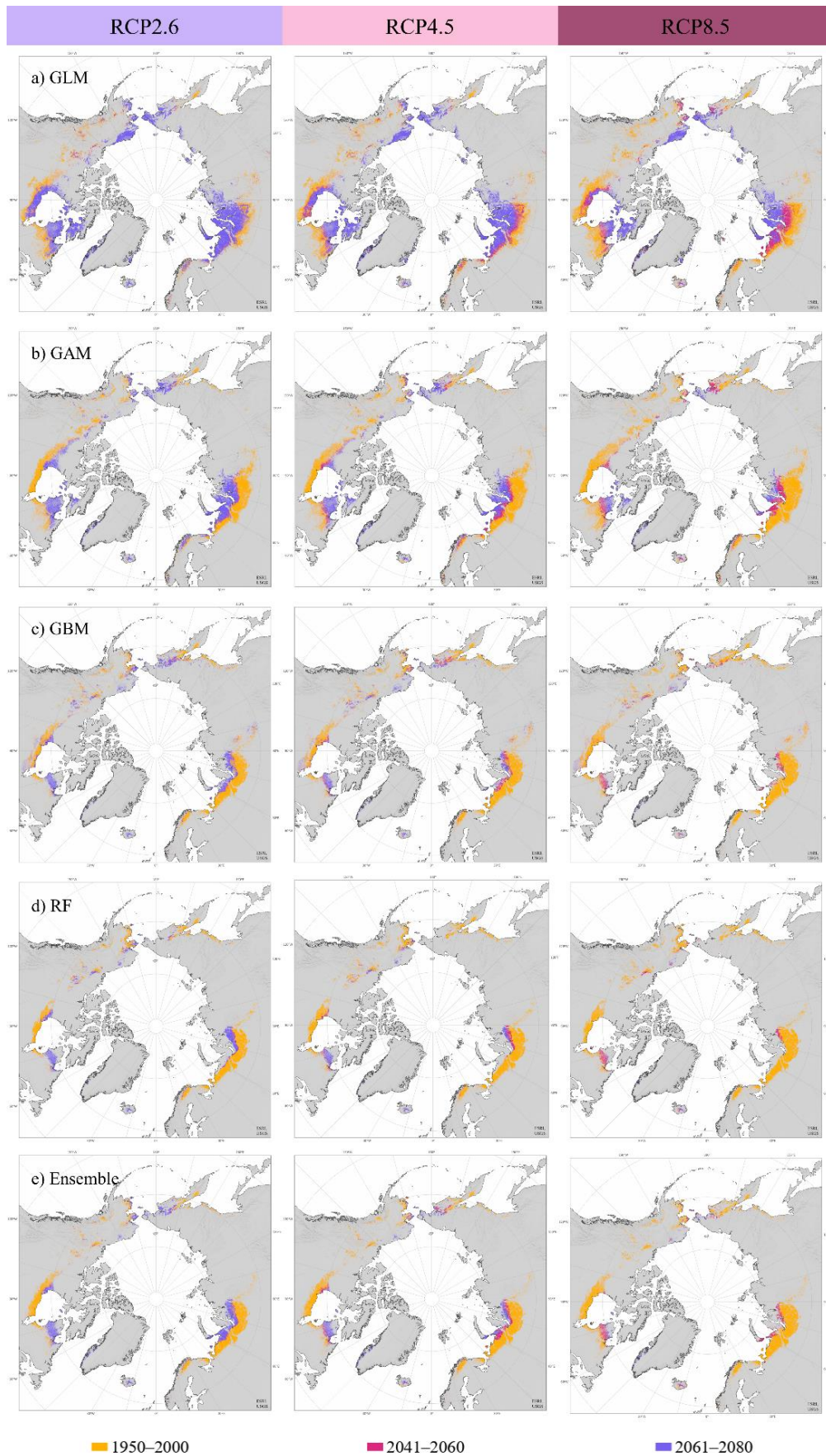


**Figure S6: Predicted changes in distribution of suitable environmental spaces for palsas and peat plateaus for time periods 1950–2000, 2041–2060 and 2061–2080 under low (RCP2.6), moderate (RCP4.5), and high emissions (RCP8.5) representative concentration pathway climate change scenarios (RCP). Modelling results are presented for used modelling methods, generalized linear model (GLM; a), generalized additive model (GAM; b), generalized boosting method (GBM; c), random forest (RF; d), and ensemble (e) of the former methods. Results are provided for the permafrost region (Ran et al. 2022) and for the future periods for the extent of the period 1950–2000.**

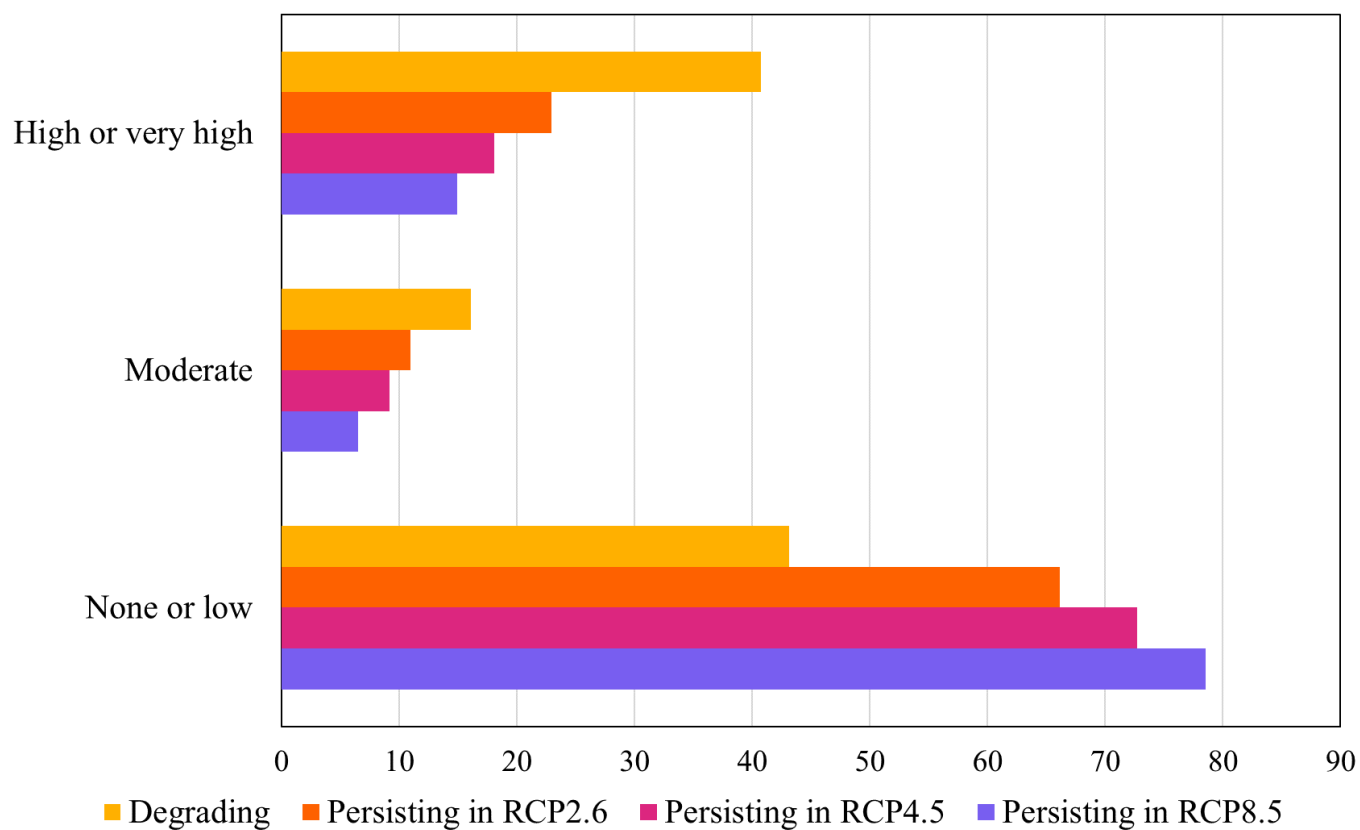


**Figure S7: Classified wetland thermokarst likelihoods (%)**, Olefeldt et al., 2016) of the regions that our models predicted to be lost (under RCP2.6) and persist as suitable palsa and peat plateau environments during the period 2040–2061 in RCP2.6, RCP4.5, and RCP8.5 climate change scenarios.



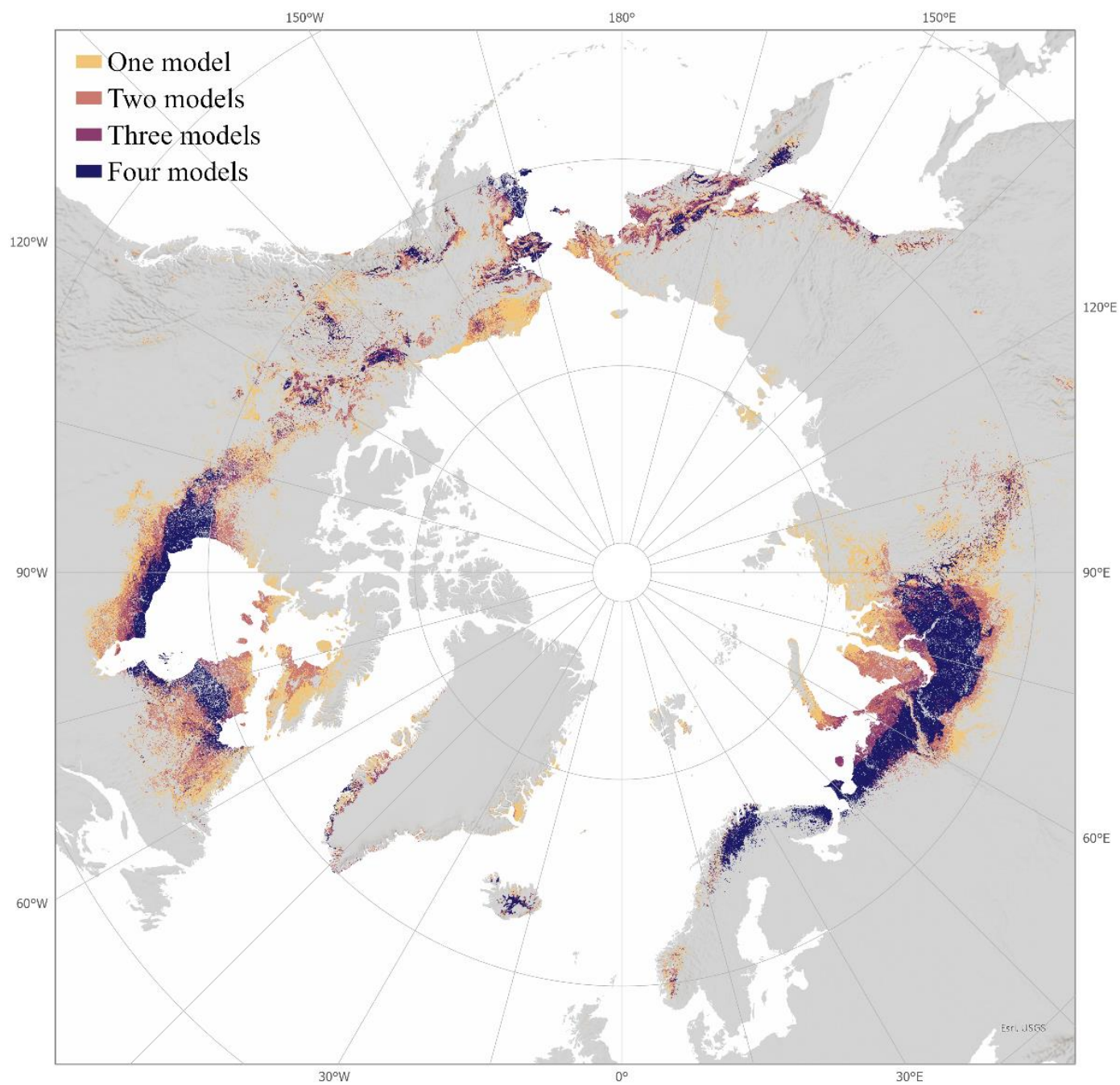


**Figure S8: Inter-model variability in predicted suitable environmental spaces for palsa mires in 1950–2000. The model agreement from low (one model predicts palsa occurrence) to high (all four models predict palsa occurrence) is illustrated with graded colors from yellow to dark blue. Results are provided for the permafrost region (Ran et al., 2022).**